

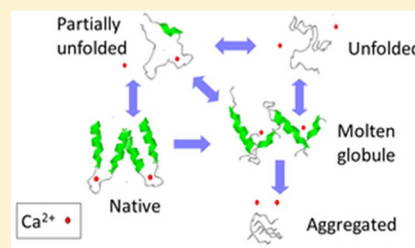
# Pressure–Temperature Stability, $\text{Ca}^{2+}$ Binding, and Pressure–Temperature Phase Diagram of Cod Parvalbumin: Gad m 1

Judit Somkuti,<sup>†</sup> Merima Bublin,<sup>‡</sup> Heimo Breiteneder,<sup>‡</sup> and László Smeller<sup>\*,†</sup>

<sup>†</sup>Department of Biophysics and Radiation Biology, Semmelweis University, Budapest, Hungary

<sup>‡</sup>Department of Pathophysiology and Allergy Research, Medical University of Vienna, Vienna, Austria

**ABSTRACT:** Fish allergy is associated with IgE-mediated hypersensitivity reactions to parvalbumins, which are small calcium-binding muscle proteins and represent the major and sole allergens for 95% of fish-allergic patients. We performed Fourier transform infrared and tryptophan fluorescence spectroscopy to explore the pressure–temperature ( $p$ – $T$ ) phase diagram of cod parvalbumin (Gad m 1) and to elucidate possible new ways of pressure–temperature inactivation of this food allergen. Besides the secondary structure of the protein, the  $\text{Ca}^{2+}$  binding to aspartic and glutamic acid residues was detected. The phase diagram was found to be quite complex, containing partially unfolded and molten globule states. The  $\text{Ca}^{2+}$  ions were essential for the formation of the native structure. A molten globule conformation appears at 50 °C and atmospheric pressure, which converts into an unordered aggregated state at 75 °C. At >200 MPa, only heat unfolding, but no aggregation, was observed. A pressure of 500 MPa leads to a partially unfolded state at 27 °C. The complete pressure unfolding could only be reached at an elevated temperature (40 °C) and pressure (1.14 GPa). A strong correlation was found between  $\text{Ca}^{2+}$  binding and the protein conformation. The partially unfolded state was reversibly refolded. The completely unfolded molecule, however, from which  $\text{Ca}^{2+}$  was released, could not refold. The heat-unfolded protein was trapped either in the aggregated state or in the molten globule state without aggregation at elevated pressures. The heat-treated and the combined heat- and pressure-treated protein samples were tested with sera of allergic patients, but no change in allergenicity was found.



Fish plays an especially important role in healthy nutrition because it is a valuable source of proteins, omega-3 polyunsaturated fatty acids, and fat-soluble vitamins. Considering enhanced fish production and an increase in its consumption, the recently determined 2% prevalence of fish allergy is expected to increase in the future.<sup>1–3</sup>

The major fish allergen parvalbumin represents an extremely abundant allergen in many fish species,<sup>4</sup> and the calcium-bound form has been shown to be remarkably stable.<sup>5,6</sup> Boiling and cooking fish can also lead to the formation of molecular aggregates and enhancement of IgE reactivity as shown for tuna, salmon, cod, flounder, and whiff.<sup>6,7</sup> Parvalbumin is usually found in the white muscle of fish<sup>8</sup> where it is responsible for the relaxation of muscle fibers. The structure of the parvalbumin from carp was first determined by Kretsinger and Nockolds in 1973, which was the first EF-hand motif described.<sup>9</sup> Gad m 1 is the major allergen of Atlantic cod (*Gadus morhua*).<sup>10</sup>

Gad m 1.01 consists of 109 amino acids. Although the crystal structure of Gad m 1 is not known, our homology modeling study showed that the molecule has a globular shape with six short helices and two active  $\text{Ca}^{2+}$ -binding sites (Figure 1). Parvalbumin can be regarded as a model  $\text{Ca}^{2+}$ -binding protein. It is a member of the EF-hand protein family containing a helix–loop–helix sequence of ~30 amino acids. EF-hand  $\text{Ca}^{2+}$ -binding proteins have many important functions such as muscle contraction,<sup>11</sup> calcium buffering in the cytosol,<sup>12</sup> and signal transduction between cellular compartments.<sup>13</sup> As calcium can regulate the function of these proteins, it is important to know how the  $\text{Ca}^{2+}$  ions are bound in the different phases.

Application of high pressure is a rapidly developing field in protein biophysics and food technology.<sup>14–18</sup> From a thermodynamic point of view, pressure is a thermodynamic parameter that is as important as temperature, but less widely studied mainly because of experimental difficulties. Pressure experiments can reveal other important thermodynamic parameters of the systems, mostly those connected to volume changes.<sup>19,20</sup> Proteins require sufficient conformational flexibility for their functions, and therefore, they are only marginally stable; i.e., the native state exists only within a particular pressure–temperature range under given solvent conditions. It is well-known that pressure can act on proteins affecting their enzymatic activity and quaternary, tertiary, and even secondary structure.<sup>21–23</sup> Pressure has a pronounced effect on the aggregation behavior of proteins as well.<sup>24–26</sup> A relatively low pressure of 100–200 MPa is usually enough to dissociate oligomers and in some cases aggregates.<sup>20,27</sup> Higher pressures (0.5–1 GPa) can cause denaturation of the protein.<sup>28,29</sup> The conformations adopted by the protein under different pressure and temperature conditions can be presented in a  $p$ – $T$  (pressure–temperature) phase diagram. The classical form of the diagram has an elliptic denaturation boundary, but recently, the diagram has been generalized and extended by metastable

Received: March 29, 2012

Revised: June 21, 2012

Published: July 5, 2012



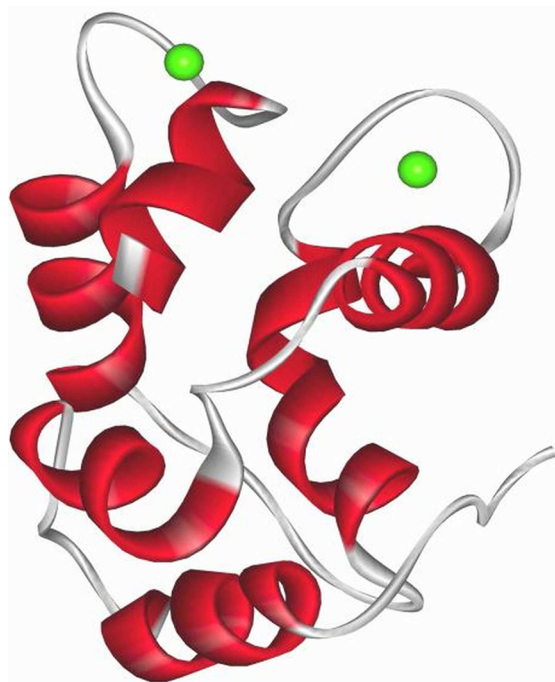


**Figure 1.** Ribbon diagram of the homology model structure of Gad m 1 (green spheres are  $\text{Ca}^{2+}$ ).

states to include intermediate and aggregated states of the proteins.<sup>30</sup>

Studies of proteins in solution reported pressure-induced unfolding in the range of 0.2–1 GPa depending on the actual protein. The typical unfolding pressure under the physiological solution and temperature conditions is around 500 MPa.<sup>31–33</sup> Application of high pressure in the food industry is also becoming accepted as a replacement for heat treatment. This is advantageous because it is a gentle treatment with regard to nutrients and vitamins and can also increase the shelf life of products by inactivating bacteria.

Recently, pressure treatment was successfully applied to unfold Mal d 1, an allergenic protein from apple.<sup>34–37</sup> Our previous high-pressure FTIR (Fourier transform infrared) spectroscopy study<sup>38</sup> showed an irreversible unfolding of Mal d 1 followed by the aggregation of the protein.

The main aim of this study was to reveal the pressure–temperature phase diagram of the major cod allergen Gad m 1 to investigate the possibility of its inactivation. We wanted to conduct a detailed study of secondary structure changes of the protein as a function of pressure and temperature, thus elucidating the nature of the phase transitions leading to the completely unfolded state. The characterization of the intermediate states and the aggregation of the protein were also very important from the point of view of irreversibility, which is a prerequisite for inactivation.

We used *in situ* high-pressure infrared spectroscopy to follow secondary structure changes and aggregation simultaneously. The most important information provided by the infrared spectrum resides in the amide I band.<sup>39</sup> This involves mainly the carbonyl stretching vibrations of the peptide backbone. Different secondary structures result in quite different amide I bands. The relative abundance of the secondary structure types can be obtained from the analysis of the amide I band.<sup>40–42</sup> The amide II band reports on H/D exchange. Consequently, it gives information about flexibility. In the case of parvalbumin, we

also took advantage of the  $\text{COO}^-$  antisymmetric stretching vibration that was ideal for monitoring the  $\text{Ca}^{2+}$  binding of the protein.<sup>43,44</sup>

Investigating purified proteins can improve the biochemical, biophysical, and immunological characterization of food allergens, which is important in understanding the structural components of allergenicity and will open new perspectives for producing weakly allergenic or nonallergenic processed foods. If the exact structure of parvalbumin is essential for triggering the allergic reaction, we expect a reduced level of IgE binding after denaturation of the protein by pressure or temperature treatment. From the  $p$ – $T$  phase diagram, we can see which pressure–temperature coordinates are appropriate for denaturing the protein. If only the conformational epitopes are responsible for the allergenicity, denaturing the protein will not necessarily change the allergenicity.

## MATERIALS AND METHODS

**Purification of Gad m 1.** Atlantic cod (*G. morhua*) muscle was homogenized with 3 volumes of extraction buffer containing 20 mM Bis-Tris {2-[bis(2-hydroxyethyl)amino]-2-(hydroxymethyl)-1,3-propanediol}/HCl (pH 7) and 3 mM  $\text{NaN}_3$ . Proteins were extracted by stirring the homogenate for 3 h at 4 °C. After centrifugation, the supernatant was collected and filtered through Miracloth and filter papers, subsequently, to remove cellular debris. The clear solution was applied to a DEAE (diethylaminoethanol) Sepharose column. After the solution had been washed with binding buffer [20 mM Bis-Tris/HCl (pH 7)], elution of bound protein was achieved by a linear gradient from 0 to 25% elution buffer [20 mM Bis-Tris/HCl (pH 7) and 1 M NaCl]. Selected fractions were then loaded onto a gel filtration column. Fractions containing parvalbumin (Gad m 1.01) were dialyzed against 20 mM Tris/HCl buffer and stored at –20 °C. The purified protein was dialyzed against distilled water before lyophilization.

**Infrared Spectroscopy.** For the infrared spectroscopic measurements, the sample was dissolved at a concentration of 75 mg/mL in a  $\text{D}_2\text{O}$  buffer containing 1 M Bis-Tris (pD 7) and 0.2 M  $\text{CaCl}_2$ . Heavy water ( $\text{D}_2\text{O}$ ) was used because  $\text{H}_2\text{O}$  has a strong absorption peak at  $1640\text{ cm}^{-1}$ , which obscures the amide I band. The infrared spectra were recorded with a Bruker Vertex80v (Bruker Optics, Billerica, MA) FTIR spectrometer equipped with a high-sensitivity MCT (mercury–cadmium–telluride) detector. Each spectrum was collected by averaging 256 scans at  $2\text{ cm}^{-1}$  resolution. The infrared beam was focused on a high-pressure diamond anvil cell (Diacell, Leichesters, U.K.) using a Bruker AS25 type beam condenser. The diamond cell was allowed to reach a pressure of 1.6 GPa under controlled temperature conditions.  $\text{BaSO}_4$  was used as internal calibrant to determine the pressure.<sup>45</sup> The sample temperature was controlled with a Eurotherm controller (type 2216e) and measured with a thermocouple (OMEGA Engineering, Stamford, CT). The heating rate was  $0.2\text{ °C/min}$ .

The pressure- and temperature-induced transitions were fit with a two-state transition model.<sup>38</sup>

Infrared spectra were deconvoluted using OPUS (Bruker) with the following parameters: Lorentzian band shape, bandwidth of  $5.2\text{ cm}^{-1}$ , and resolution enhancement factor of 1.84. Deconvoluted spectra were fit using Gaussian component bands to obtain the abundance of the secondary structure elements.<sup>41,46,47</sup>

**Fluorescence Spectroscopy.** Fluorescence spectra were recorded with a Fluorolog-3 (Horiba Jobin Yvon) spectrometer

equipped with a homemade temperature controller. Fluorescence spectra were recorded for Gad m 1 as a function of temperature up to 89 °C. Samples were excited at 290 nm, and emission was collected at 300–450 nm at 2 nm resolution. The protein concentration was 50 times lower than in the infrared measurements.

**Homology-Based Model of Gad m 1.** Homology modeling was performed with the Swissmodel Protein Modeling Server<sup>48–50</sup> using the structure of whiting parvalbumin (1a75B) as a template.

**IgE Enzyme-Linked Immunosorbent Assay (ELISA).** Samples were treated in a glass tube sealed with a rubber stopper. The tube was placed in a thermostated high-pressure cell (U-103, Unipress, Warsaw, Poland). The pressure was increased with a Nova Swiss hand pump. Water was used as the pressure transmitting medium. For the ELISA experiment, microtiter plates were coated with 1 µg of untreated, heat-treated (80 °C), or pressure- and heat-treated Ca<sup>2+</sup>-bound cod parvalbumin per well. After the sample had been blocked with Tris-buffered saline (TBS) containing 0.5% (v/v) Tween 20 and 3% (w/v) nonfat dry milk, 1:4 diluted individual sera from fish allergic patients were applied to the plates and the plates incubated overnight at 4 °C. After being washed, the plates were incubated with a 1:1000 diluted alkaline phosphatase-conjugated mouse anti-human IgE antibody (BD Pharmingen, San Diego, CA) for 2 h at room temperature. Color development was performed using disodium *p*-nitrophenyl phosphate substrate tablets (Sigma-Aldrich, Steinheim, Germany), and the optical density (OD) was measured at 405 nm. Three sera of nonallergic subjects were used as negative controls. OD values were counted positive if they exceeded the mean OD of the negative controls by more than three standard deviations.

## RESULTS

### Effect of Ca<sup>2+</sup> Ions on the Structure of Gad m 1 Parvalbumin under Ambient Conditions. Figure 2 (curve

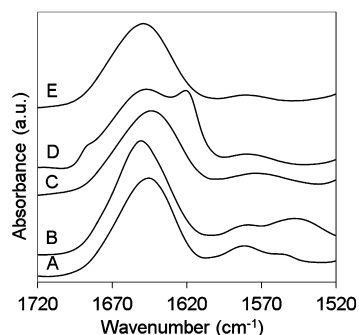


**Figure 2.** FTIR spectra of a 75 mg/mL Gad m 1 solution in 1 M Bis-Tris at pD 7: (A) without added Ca<sup>2+</sup> at 27 °C and ambient pressure, (B) with 0.2 M CaCl<sub>2</sub> at 27 °C and ambient pressure, (C) with 0.2 M CaCl<sub>2</sub> at 40 °C and 1.6 GPa, (D) with 0.2 M CaCl<sub>2</sub> at 90 °C and ambient pressure, (E) with 0.2 M CaCl<sub>2</sub> at 90 °C and 200 MPa.

B) shows the amide I, amide II, and COO<sup>−</sup> absorption band region of the spectrum of parvalbumin in a deuterated water solution (pD 7, 0.2 M CaCl<sub>2</sub>) under ambient conditions. The protein has mainly  $\alpha$ -helical conformation, which can be seen from the maximal position (1652 cm<sup>−1</sup>) of the amide I band. The fit of the deconvoluted amide I band results in 50% helical, 16% disordered, and 34% loop content for the native state

(Table 1). These values are in good agreement with our homology modeling results, in which 54 of 109 amino acids

**Table 1. Fitted Values for the Secondary Structures Present in the Different States of Gad m 1 Determined from the Fitting of the Deconvoluted Amide I Band of the Infrared Spectrum Using Gaussian Components<sup>41,46,47</sup>**

protein phase	$\alpha$ -helix (%)	loops and turns (%)	disordered (%)	intermolecular $\beta$ -sheet (%)
native (N)	50	34	16	—
molten globule (MG)	23	43	34	—
partially unfolded (U')	4	32	64	—
unfolded (U)	—	17	83	—
aggregated (A)	—	2	73	25
Ca <sup>2+</sup> -depleted under ambient conditions	5	29	66	—
Ca <sup>2+</sup> -depleted at high pressures	—	18	82	—

contribute to helical structures and the helices are connected by large loops. The amide II band is weak but visible at 1546 cm<sup>−1</sup>. It overlaps with the antisymmetric stretching band of the COO<sup>−</sup> groups, giving a broad band at 1549 cm<sup>−1</sup>. The presence of the amide II band also indicates that the protein has its folded structure, where the hydrogens in the protein interior are not accessible to water; therefore, they are not exchanged during the time between the preparation of the solution and the first measurement. The peak at 1583 cm<sup>−1</sup> and part of the peak at 1549 cm<sup>−1</sup> come from the antisymmetric stretching vibrations of the COO<sup>−</sup> groups of glutamic and aspartic acid residues, respectively. The 1549 cm<sup>−1</sup> peak can be separated by deconvolution into two components: the amide II band appears at 1546 cm<sup>−1</sup>, although the COO<sup>−</sup> component is at 1553 cm<sup>−1</sup>. The latter can be attributed to the bidentate Ca<sup>2+</sup>-bound COO<sup>−</sup> groups of the glutamic acid residues.<sup>44</sup> Because the absorption band of the bound COO<sup>−</sup> overlaps with the amide II band, it is difficult to estimate the ratio of the contributions from the bound and free carboxylic acids from the spectrum.

The infrared band of Gad m 1 parvalbumin shows a broad amide I band with a maximal position of 1646 cm<sup>−1</sup>, in the absence of Ca<sup>2+</sup> (Figure 2A). This position and also the fitting results (Table 1) indicate a dominantly unordered rather than folded helical structure. The loss of the amide II peak in the case of the Ca<sup>2+</sup>-depleted protein indicates also the absence of a rigid inner core. In the Ca<sup>2+</sup>-depleted protein, all exchangeable hydrogens can be reached by the solvent during the first minutes of the sample preparation, indicating that there are no buried hydrogens. The amide band of the infrared spectrum underwent a further broadening transition at 200 MPa. The fitted amide I band indicates an unfolded structure above 200 MPa (Table 1). No further conformational transitions were found in this sample up to 1.1 GPa.

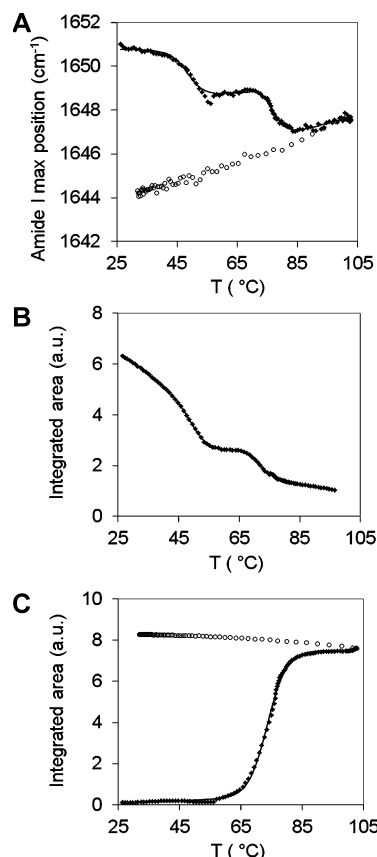
**The *p*–*T* Diagram of Ca<sup>2+</sup>-Bound Gad m 1 Parvalbumin. Temperature Unfolding.** All the following experiments were conducted with the protein containing Ca<sup>2+</sup>, which was ensured by the addition of 200 mM CaCl<sub>2</sub> to the solution.

Figure 2D shows the characteristic infrared bands at high temperatures. Both the maximal position (1647 cm<sup>−1</sup>) and the fitting results show that the majority (73%) of the protein is unfolded (Table 1). The peaks at 1618 and 1688 cm<sup>−1</sup> are specific for intermolecular antiparallel  $\beta$ -sheets<sup>51</sup> and show that 25% of the amino acids take part in the stabilization of the



aggregates at 90 °C, which is well above the unfolding temperature.

Looking at the characteristic spectrum features (maximal position of peaks, peak width, and integrated area under peaks) as a function of temperature, we can find two transitions (Figure 3). At the first transition, the amide II band disappears



**Figure 3.** Temperature denaturation of Gad m 1: (A) amide I band maximal position, (B) integrated area under the COO<sup>−</sup> and amide II peaks, and (C) integrated area under the peak at 1619 cm<sup>−1</sup> (aggregation peak) as a function of temperature [(♦) forward, (○) backward, and (—) fitted sigmoid curves].

and a small shift in the amide I band position can be observed. Curve fitting to the deconvoluted spectra shows a decrease in the helical content and an increase in the disordered and loop content (Table 1). At 75 °C, the amide I band position shifts further to the value characteristic of the unordered conformation. Following the area of the aggregation band at 1618 cm<sup>−1</sup>, we obtained a sigmoid curve, which shows a slightly lower transition point (73.5 °C) compared to that of the amide I maximal position. As one can see in panels A and C of Figure 3, both the unfolding transition and the aggregation are irreversible.

We investigated the heat denaturation at different pressures. Performing the temperature experiment at 200 MPa, we observed both of the transitions that can be detected without pressure, and unfolded protein structure was clearly identified above the second transition (Table 1). The increased pressure, however, prevented the unfolded protein from aggregating (Figure 2E). Also, the temperatures of the two transitions were considerably lower (40 and 62.5 °C) compared to the values observed at ambient pressure.

We also followed temperature unfolding at atmospheric pressure by fluorescence spectroscopy, using as a reporter the tryptophan residue of the protein. The maximal position of the emission spectrum shifts to higher wavelengths in two steps. The first transition has nearly the same midpoint (49.2 °C) (Figure 4) as in the case of the infrared measurements (50 °C).

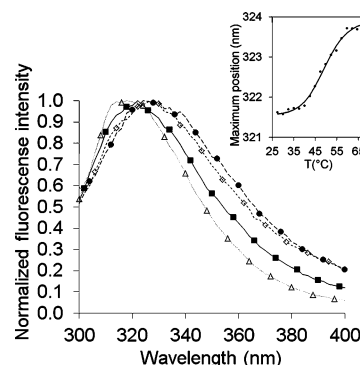


**Figure 4.** Normalized fluorescence intensity of Gad m 1 at ambient pressure and 30 (△), 67 (■), and 89 °C (●) and 30 °C after the treatment (◇). The inset shows the maximal position of the fluorescence spectra of Gad m 1 as a function of temperature.

At the temperature of the unfolding transition, irreversible changes took place in the spectra. Neither the maximal position nor the signal amplitude returned to the original value after the sample had been cooled to room temperature.

**Pressure Unfolding.** Around room temperature (27 °C), we can see one transition at 520 MPa. The amide I band becomes broader at this pressure (Figure 5), and the amide II band

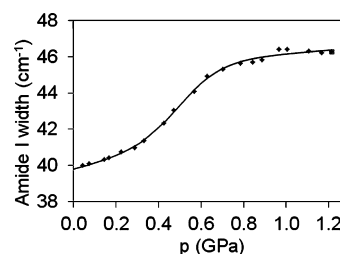


**Figure 5.** Pressure-induced transition of Gad m 1. Width of the amide I band as a function of pressure.

disappears. Simultaneously, the amide I band shifts from the  $\alpha$ -helical position (1652 cm<sup>−1</sup>) toward lower wavenumbers. Although the plot of the amide I position versus pressure does not show a steplike character, this can be understood from the complex nature of the amide band that consists of several overlapping bands characteristic of different secondary structures in the proteins. The position of the amide I band above the transition is somewhere between the wavenumbers characteristic of  $\alpha$ -helical and unfolded conformations. It has to be noted that the maximal position of the amide I peak shifts further above 520 MPa, approaching the value characteristic of the unfolded protein. This suggests that the protein loses most of its remaining structural elements at pressures between 520 and 1200 MPa. This is supported by the fitting results, showing a small amount remained helical and an increased loop content besides the major unfolded component (Table 1). At 40 °C, we found the same transition with a slightly different transition pressure: the midpoint of the broadening of the amide I band is

at 480 MPa. The amide I maximal position shows a sigmoidlike transition at this temperature too, but the transition pressure is slightly lower than that obtained from the bandwidth. Above this transition, the maximal position shifts further and after a second transition at 1.14 GPa reaches  $1644\text{ cm}^{-1}$ , characteristic of the totally structureless unfolded state, containing only a small amount of loops besides the disordered chain (Table 1). At  $55\text{ }^{\circ}\text{C}$ , the pressure of the first transition is at 220 MPa. At this temperature, we start the pressure experiment already from a molten globule phase because we are above the first temperature transition [ $50\text{ }^{\circ}\text{C}$  (see the previous section)]. A second transition to the completely unfolded state can be seen at 890 MPa.

**$\text{Ca}^{2+}$  Binding in the Different Conformations.** Figure 6 shows the antisymmetric stretching mode vibrations of the

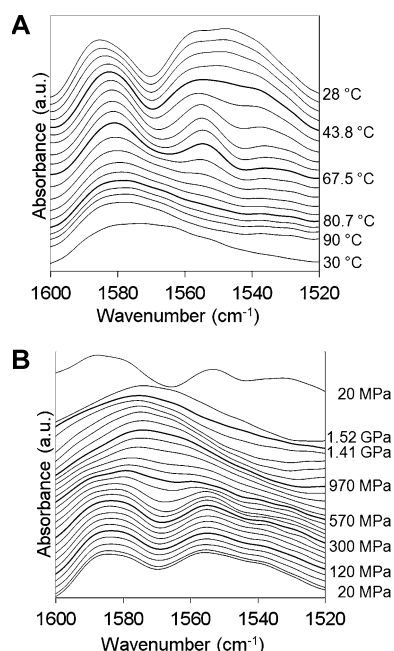


**Figure 6.** Deconvoluted FTIR spectra of the  $\text{COO}^-$  band region of Gad m 1. (A)  $T = 27\text{ }^{\circ}\text{C}$ . Pressures from bottom to top: 20, 40, 45, 95, 120, 145, 180, 215, 270, 300, 350, 380, 440, 510, 570, 655, 710, 810, 890, 970, 1065, 1140, 1210, 1380, 1410, 1520, and 20 MPa backward. (B) At ambient pressure. Temperatures from top to bottom: 28, 29.8, 34.3, 39, 43.8, 48.5, 53.3, 58.1, 62.8, 67.5, 71.9, 75.4, 76.9, 78.6, 80.7, 83.5, 87.7, 90, and  $30\text{ }^{\circ}\text{C}$  backward.

$\text{COO}^-$  group that are sensitive to  $\text{Ca}^{2+}$  binding. The deconvoluted spectra of the pressure experiment at  $40\text{ }^{\circ}\text{C}$  can be seen in Figure 6A. The  $1554\text{ cm}^{-1}$  peak corresponds to the bidentate binding of  $\text{Ca}^{2+}$  to the Glu residues. This is slightly higher than the value of  $1553\text{ cm}^{-1}$  found by Nara and Tanokura,<sup>44</sup> but the shift can be explained by the slightly higher temperature ( $40\text{ }^{\circ}\text{C}$  in our case compared to room temperature in their experiments). The broad feature at lower wavenumbers corresponds to the remainder of the amide II band. The  $1585\text{ cm}^{-1}$  band consists of two vibrations ( $1579$  and  $1590\text{ cm}^{-1}$ ), which can be separated only by stronger deconvolution or second-derivative peak determination. These reflect the vibrations of the aspartic acid residues. It is known that the frequency of the  $\text{COO}^-$  antisymmetric vibration downshifts because of a bidentate binding, although the unidentate binding causes an increase in frequency compared to that of the free state.<sup>52</sup> We assign therefore the higher component to the

unidentate binding of the  $\text{Ca}^{2+}$  and the lower component to the free aspartic acid residue. It has to be also noted that the free aspartic acid in the middle of a folded protein does not necessarily have the same vibrational frequency as the free aspartic acid in an aqueous environment. The same applies for the  $\text{COO}^-$  group of the glutamic acid residues. A closer look at the three-dimensional (3D) structure arising from the homology modeling shows that many of these residues are able to bind to other charged residues or create a hydrogen bond inside the protein, which makes the signal of the “free”  $\text{COO}^-$  groups unpredictable. During the transition at 480 MPa, the intensity of the  $1590\text{ cm}^{-1}$  component decreases and that of the  $1579\text{ cm}^{-1}$  component increases. Simultaneously, the intensity of the  $1554\text{ cm}^{-1}$  band decreases and the absorbance increases at  $1565\text{ cm}^{-1}$ , which is known to be characteristic of the free glutamic acid residues. At the highest pressures ( $>1.14\text{ GPa}$ ), the  $\text{COO}^-$  region shows one band at  $1573\text{ cm}^{-1}$ , which can be decomposed by deconvolution to the components at  $1565$  and  $1575\text{ cm}^{-1}$ , both characteristic of the free residues. This is consistent with the above finding that the protein reaches the fully denatured state only at 1.14 GPa.

During the temperature experiment at atmospheric pressure, we can clearly see the disappearance of the amide II peak at  $50\text{ }^{\circ}\text{C}$  (Figure 6B). Above this temperature, the protein retains a molten globule structure. In this state, a strong absorption band was observed at  $1553\text{ cm}^{-1}$ , which shows that the  $\text{Ca}^{2+}$  ions are connected to the Glu residues by a bidentate coordination. The  $\text{COO}^-$  vibration of the aspartic acid is shifted, however, toward lower wavenumbers, indicating the loosening of the binding site. This peak disappears at the heat unfolding temperature ( $75\text{ }^{\circ}\text{C}$ ). Simultaneously, the absorbance increases at  $1565\text{ cm}^{-1}$ , characteristic of the free glutamic acid residues. The peak reflecting the aspartic acid binding also changes during the temperature experiment. The amount of the free component at  $1576\text{ cm}^{-1}$  increases in two steps during the two transitions.

**Reversibility.** After a pressure cycle at  $27\text{ }^{\circ}\text{C}$ , the protein rebinds  $\text{Ca}^{2+}$  when returning from the partially unfolded state. The amide I position is equal to the initial value, indicating the refolding of the protein. At  $40\text{ }^{\circ}\text{C}$ , returning from the totally denatured state, the protein does not regain its initial structure: neither the conformation nor the  $\text{Ca}^{2+}$  binding is fully reversible. Both the position of the amide I band and the  $\text{COO}^-$  region of the spectrum resemble those of the  $\text{Ca}^{2+}$ -depleted protein. The protein did not rebound  $\text{Ca}^{2+}$  after a heat cycle when aggregation took place. The protein unfolded at 200 MPa did partially refold and rebound the  $\text{Ca}^{2+}$  again, resembling the  $\text{Ca}^{2+}$ -depleted case.

If the heat cycle reaches only  $55\text{ }^{\circ}\text{C}$ , where the molten globule structure can be found, neither the structure nor the  $\text{Ca}^{2+}$  binding is reversible. The protein again resembled the  $\text{Ca}^{2+}$ -depleted case, which is highly similar to the molten globule state itself.

**Allergenicity Test.** Three samples were tested for IgE binding by an ELISA using sera from six fish-allergic patients: (1) untreated control, (2) heat-treated serum ( $80\text{ }^{\circ}\text{C}$  for 30 min) at atmospheric pressure, and (3) heat-treated serum at a high pressure ( $80\text{ }^{\circ}\text{C}$  and 0.3 GPa). In this last case, the sample was pressurized to 300 MPa, heated to  $80\text{ }^{\circ}\text{C}$ , kept there for 30 min, cooled (still under pressure) to  $30\text{ }^{\circ}\text{C}$ , and depressurized. Compared to the untreated allergen, the treated protein exhibited neither weakened nor enhanced IgE binding (Figure 7).

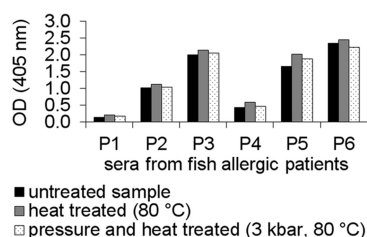


**Figure 7.** IgE reactivity of six fish-allergic patients to untreated, heat-treated (80 °C), or pressure- and heat-treated cod parvalbumin. IgE binding was assessed by an ELISA.

## DISCUSSION

**Effect of  $\text{Ca}^{2+}$  Ions on the Structure of Gad m 1 Parvalbumin under Ambient Conditions.** The predominantly  $\alpha$ -helical secondary structure obtained from the analysis of the FTIR spectra agrees well with the structure obtained by homology modeling.

Because parvalbumin binds two  $\text{Ca}^{2+}$  ions in its native state, it is an interesting question the extent to which this structure is destabilized in the absence of the  $\text{Ca}^{2+}$  ions. Analyses of the amide I and II bands (Figure 2A,B and Table 1) show that the protein structure is less ordered in the absence of  $\text{Ca}^{2+}$  ions. Besides the smaller amount of the ordered structures, a loosening of the tertiary structure is indicated by the absence of the amide II band for the  $\text{Ca}^{2+}$ -depleted protein. Permyakov et al. also observed that the  $\text{Ca}^{2+}$ -depleted pike parvalbumin was in an unordered state.<sup>53</sup> There is, however, a sign that this structure was not a completely unordered one because a transition with further broadening was observed at 200 MPa. Because of this fact and the fitted results (Table 1), we concluded that the sample without addition of  $\text{Ca}^{2+}$  is in a partially unordered state containing traces of ordered structure, which are lost at 200 MPa. Similar behavior was reported in the case of troponin C in which the apo state was denatured by a quite low pressure (<100 MPa), but higher hydrostatic pressure combined with urea was needed to denature the  $\text{Ca}^{2+}$ -bound protein.<sup>54–56</sup>

**Temperature Unfolding.** The first transition at 50 °C leads to a molten globule structure. The flexibility of the protein increases during this transition, which can be judged both from the fitting results and from the disappearance of the amide II band. The amount of loops and turns also increased, and H/D exchange was completed here because of a loosening of the tertiary structure, which made the protein interior accessible for the solvent. This is also supported by the tryptophan fluorescence measurements showing a transition toward longer emission wavelengths at the same temperature. The protein has a single tryptophan residue, which is in the middle of the folded structure according to homology modeling. This buried state is confirmed by the low emission maximal position (322 nm). The red shift above 50 °C means an increase in the polarity of the protein interior, indicating the loosening of the tertiary structure, i.e., appearance of a molten globule structure in accordance with the infrared results. Because the transition temperatures are the same within the experimental error in the infrared and fluorescence experiments, we can conclude that in this transition the concentration of the protein does not play any role. The 50-fold higher concentration in the infrared spectroscopic measurements could influence the transition only if intermolecular interactions were involved. In the native to molten globule transition,

however, only the internal conformation of the protein changes; therefore, this transition is concentration-independent. Similar consideration applies for the other transitions, which do not involve aggregation of the protein.

The denaturation at 75 °C is accompanied by aggregation of the protein. The lower transition temperature of the aggregation process compared to the secondary structure changes can be explained by a strong interaction between the unfolding and aggregation processes. The loosened structure of the molten globule allows some hydrophobic surfaces to be exposed to the solvent. These hydrophobic surfaces could initiate the aggregation of the protein, when they have lost their secondary structure at high temperatures. This is enough to trigger the nucleation, but unfolding of all of the proteins is needed for the completion of aggregation. The fluorescence experiments show slightly higher unfolding temperatures than infrared absorption. This is a result of a slower aggregation in the samples that contained a 50-fold lower protein concentration. This temperature shift also supports the idea of the strong coupling between unfolding and aggregation. Fitting of the sigmoid curves described in Materials and Methods assumes a reversible transition, while both unfolding and aggregation are irreversible. This is why the fitted transition  $\Delta H$  values are not used in the analysis.

Pressure influences the intermolecular interactions strongly; therefore, studying temperature-induced denaturation at elevated pressures is of special interest. Pressure was shown to prevent aggregation,<sup>26,57</sup> which is characteristic of the heat denaturation at ambient pressure. Performing the heat treatment at >200 MPa allowed us to achieve the true unfolded state of the protein without it being disturbed by aggregation (Table 1).

**Pressure Unfolding.** There are many debates about whether a pressure-unfolded protein loses its secondary structure completely or whether secondary structure elements remain in the pressure-unfolded form.<sup>28,58</sup> According to our measurements, although the majority of the secondary structure was lost, a completely unfolded state could not be reached at room temperature. As one can see from the position of the amide I band, this partially unfolded state is drifting toward the direction of the completely unfolded one, but the completely unfolded state is not reached at room temperature. The solidification of water happens at room temperature around 1 GPa in pure water, while between 1 and 1.5 GPa for protein solutions depending on the type and concentration of the protein limiting the achievable pressure range. Fortunately, the freezing pressure of water increases with temperature (not shown), which allows higher pressures to be reached in the liquid phase at higher temperatures. The transition to the completely unfolded state occurred at 1.14 GPa and 40 °C, and at 890 MPa and 50 °C. Using the results of the combined pressure and temperature measurements, we constructed the  $p$ – $T$  phase diagram of the protein (Figure 8). This contains a molten globule (MG) and a partially unfolded ( $U'$ ) state besides the usual native (N) and unfolded (U) states. The difference between U and  $U'$  can be shown both by the different secondary structure compositions (Table 1) and by analyzing the  $\text{Ca}^{2+}$  binding ability of the protein.

**$\text{Ca}^{2+}$  Binding in the Different Conformations.** As one can see from the FTIR spectra under ambient conditions, parvalbumin needs  $\text{Ca}^{2+}$  for its native folded structure. Parvalbumin binds the  $\text{Ca}^{2+}$  ion by the  $\text{COO}^-$  groups of its aspartic and glutamic acid side chains. There are 11 aspartic



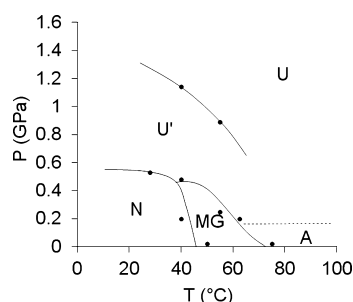


**Figure 8.** Pressure–temperature phase diagram of Gad m 1. Abbreviations: N, native; MG, molten globule; A, aggregated; U, unfolded; U', partially unfolded.

acid and 8 glutamic acid residues in the protein. The two  $\text{Ca}^{2+}$ -binding sites are composed of residues 51–63 and 91–102.<sup>5</sup> According to the 3D structure obtained from our homology modeling (Figure 1), five aspartic acids and three glutamic acids participate in  $\text{Ca}^{2+}$  binding. A similar binding pocket has been found by Nara and Tanokura<sup>44</sup> in pike parvalbumin.

Analysis of the antisymmetric vibrations of the  $\text{COO}^-$  groups leads to the conclusions that the  $\text{Ca}^{2+}$ -binding site is destabilized during the (partial) unfolding of the protein caused by pressurization. The most probable explanation is that one of the two binding sites is destroyed during the native (N)  $\rightarrow$  partially unfolded (U') transition but a certain amount of  $\text{Ca}^{2+}$  is still bound to the protein.  $\text{Ca}^{2+}$  binding to a mostly structureless protein sounds unusual, but a similar observation was reported by Dzwolak and Taniguchi for  $\alpha$ -lactalbumin.<sup>59</sup> The larger amount of loops in U' compared to the U state also supports the idea of a preserved  $\text{Ca}^{2+}$ -binding site. In the U' state, the  $\text{COO}^-$  peaks of Glu and Asp residues shift further in the direction of the wavenumbers characteristic of the free residues, indicating further distortion of the remaining binding site. Contrary to the partially unfolded U' state, in the fully unfolded state no  $\text{Ca}^{2+}$  ion is bound to the protein. This underlines the importance of the close correlation between the loss of the second  $\text{Ca}^{2+}$  ion and the total unfolding. The complete unfolding is only possible if the most strongly bound  $\text{Ca}^{2+}$  ion was released by the protein.

In the heat-induced molten globule state, both binding sites are conserved, but their distortion is clear from the change in the  $\text{COO}^-$  vibration of the aspartic acid residues, which contribute the  $\text{Ca}^{2+}$ –protein interaction by weaker, unidentate binding. At the same time, bidentate glutamic acid binding is not affected, indicating that both  $\text{Ca}^{2+}$  ions are still bound to the molten globule. In the unfolded aggregated state, the free component dominates. The same applies to the aggregation-free unfolded state at elevated pressure and temperature (>200 MPa and >75 °C).

**Reversibility.** The irreversibility of the structural changes is crucial for the inactivation of the allergen. The pressure-induced transition from the native to partially unfolded state is quite reversible. If, however, the completely unfolded structure was reached (e.g., at 40 °C), the protein cannot refold and rebind both  $\text{Ca}^{2+}$  ions and becomes trapped in the  $\text{Ca}^{2+}$ -depleted state. These differences between the reversibility of the structural changes further support our distinction between the U and U' structures.

As we pointed out earlier, the temperature-unfolded states were not reversible regardless of the presence or absence of aggregation. It is not surprising that the aggregation of the

protein is irreversible, but the reversibility of the non-aggregating denaturations depends on the actual pathway on the  $p$ – $T$  diagram. If the molten globule state is reached, the protein is trapped there; otherwise, it refolds into the  $\text{Ca}^{2+}$ -depleted form. Therefore, we can conclude that the N  $\rightarrow$  MG transition is irreversible from the point of view of both conformation and  $\text{Ca}^{2+}$  binding ability. The pressure–temperature pathways of the treatment for the allergenicity experiments were also based on the irreversibility of temperature unfolding.

**Allergenicity.** Heat-treated or pressure- and heat-treated  $\text{Ca}^{2+}$ -bound cod parvalbumin showed no reduced level of IgE binding. Although the infrared experiments showed irreversible changes for these treatments in both secondary structure and  $\text{Ca}^{2+}$  binding ability, these changes seem not be enough for reducing the allergenicity of Gad m 1. One reason could be the lower concentration used in the ELISAs or the partial refolding of the protein during the time course between the treatment and the allergenicity experiments. It has been shown<sup>60</sup> that ethylene glycol bis( $\beta$ -aminoethyl ether)- $N,N,N',N'$ -tetraacetic acid treatment of carp parvalbumin decreases the allergenic activity. This means that binding of at least one of the  $\text{Ca}^{2+}$  ions is needed for full allergenicity. In our case, the protein probably refolded partially, recovering the structure of one of the  $\text{Ca}^{2+}$ -binding sites together with the epitope.

## CONCLUSION

We determined the pressure–temperature phase diagram of Gad m 1 revealing five distinct states. Besides the normally observable native, unfolded, and aggregated states, we obtained a molten globule and a partially unfolded state possessing different  $\text{Ca}^{2+}$  binding capacities. The pressure-induced partially unfolded state appeared to be reversible, although the molten globule showed a local energy minimum conformation that does not refold to the native state. The  $\text{Ca}^{2+}$ -binding site is also distorted in the molten globule state. The  $\text{Ca}^{2+}$ -depleted protein (without addition of  $\text{Ca}^{2+}$ ) also showed a conformation with reduced stability, which has properties similar to those of the molten globule. The treated proteins exhibited neither weakened nor enhanced IgE binding.

## AUTHOR INFORMATION

### Corresponding Author

\*Tüzoltó u. 37-47, Budapest, H-1444 PF 263 Hungary. Phone: +36-20-6632110. Fax: +36-1-2666656. E-mail: laszlo.smeller@eok.sote.hu.

### Funding

J.S. and L.S. were supported by Grant 77730 from the Hungarian Scientific Research Fund.

### Notes

The authors declare no competing financial interest.

## ACKNOWLEDGMENTS

We thank Sz. Osvath for critically reading the manuscript.

## REFERENCES

- (1) Sicherer, S. H. (2011) Epidemiology of food allergy. *J. Allergy Clin. Immunol.* 127, 594–602.
- (2) Pascual, C. Y., Reche, M., Fiandor, A., Valbuena, T., Cuevas, T., and Esteban, M. M. (2008) Fish allergy in childhood. *Pediatr. Allergy Immunol.* 19, 573–579.
- (3) Failer, P. (2007) Future prospects for fish and fishery products.
- (4) Fish consumption in the European Union in 2015 and 2030, FAO

Fisheries Circular No. 972/4, Food and Agriculture Organization of the United Nations, Rome.

(4) Oneil, C., Helbling, A. A., and Lehrer, S. B. (1993) Allergic Reactions to Fish. *Clin. Rev. Allergy* 11, 183–200.

(5) Ma, Y., Griesmeier, U., Susani, M., Radauer, C., Briza, P., Erler, A., Bublin, M., Alessandri, S., Himly, M., Vazquez-Cortes, S., de Arellano, I. R. R., Vassilopoulou, E., Saxoni-Papageorgiou, P., Knulst, A. C., Fernandez-Rivas, M., Hoffmann-Sommergruber, K., and Breiteneder, H. (2008) Comparison of natural and recombinant forms of the major fish allergen parvalbumin from cod and carp. *Mol. Nutr. Food Res.* 52, S196–S207.

(6) Griesmeier, U., Bublin, M., Radauer, C., Vazquez-Cortes, S., Ma, Y., Fernandez-Rivas, M., and Breiteneder, H. (2010) Physicochemical properties and thermal stability of Lep w 1, the major allergen of whiff. *Mol. Nutr. Food Res.* 54, 861–869.

(7) Bernhiselbrodbent, J., Scanlon, S. M., and Sampson, H. A. (1992) Fish Hypersensitivity I. In vitro and Oral Challenge Results in Fish-Allergic Patients. *J. Allergy Clin. Immunol.* 89, 730–737.

(8) Kobayashi, A., Tanaka, H., Hamada, Y., Ishizaki, S., Nagashima, Y., and Shiom, K. (2006) Comparison of allergenicity and allergens between fish white and dark muscles. *Allergy* 61, 357–363.

(9) Kretsinger, R. H., and Nockolds, C. E. (1973) Carp muscle calcium-binding protein. II. Structure determination and general description. *J. Biol. Chem.* 248, 3313–3326.

(10) Das Dores, S., Chopin, C., Villaume, C., Fleurence, J., and Gueant, J. L. (2002) A new oligomeric parvalbumin allergen of Atlantic cod (Gad ml) encoded by a gene distinct from that of Gad cl. *Allergy* 57, 79–83.

(11) Holmes, K. C. (1996) Muscle proteins: Their actions and interactions. *Curr. Opin. Struct. Biol.* 6, 781–789.

(12) Skelton, N. J., Kordel, J., Akke, M., Forsen, S., and Chazin, W. J. (1994) Signal-Transduction Versus Buffering Activity in Ca<sup>2+</sup>-Binding Proteins. *Nat. Struct. Biol.* 1, 239–245.

(13) Kranz, J. K., Flynn, P. F., Fuentes, E. J., and Wand, A. J. (2002) Dissection of the pathway of molecular recognition by calmodulin. *Biochemistry* 41, 2599–2608.

(14) Panick, G., Vidugiris, G. J. A., Malessa, R., Rapp, G., Winter, R., and Royer, C. A. (1999) Exploring the temperature-pressure phase diagram of staphylococcal nuclease. *Biochemistry* 38, 4157–4164.

(15) Winter, R. (2010) Exploring the Energy and Conformational Landscape of Biomolecules under Extreme Conditions. In *High-Pressure Crystallography: From Fundamental Phenomena to Technological Applications* (Boldyreva, E., and Dera, P., Eds.) pp 573–590, Springer, Berlin.

(16) Silva, J. L., Foguel, D., and Royer, C. A. (2001) Pressure provides new insights into protein folding, dynamics and structure. *Trends Biochem. Sci.* 26, 612–618.

(17) Schroer, M. A., Paulus, M., Jeworrek, C., Krywka, C., Schmacke, S., Zhai, Y., Wieland, D. C. F., Sahle, C. J., Chimenti, M., Royer, C. A., Garcia-Moreno, B., Tolan, M., and Winter, R. (2010) High-Pressure SAXS Study of Folded and Unfolded Ensembles of Proteins. *Biophys. J.* 99, 3430–3437.

(18) Knorr, D., Froehling, A., Jaeger, H., Reineke, K., Schlueter, O., and Schoessler, K. (2011) Emerging Technologies in Food Processing. In *Annual Review of Food Science and Technology* (Doyle, M. P., and Klaenhammer, T. R., Eds.) Vol. 2, pp 203–235, Annual Reviews, Palo Alto, CA.

(19) Silva, J. L., and Weber, G. (1988) Pressure-Induced Dissociation of Brome Mosaic-Virus. *J. Mol. Biol.* 199, 149–159.

(20) Heremans, K., and Smeller, L. (1998) Protein structure and dynamics at high pressure. *Biochim. Biophys. Acta* 1386, 353–370.

(21) Herberhold, H., Royer, C. A., and Winter, R. (2004) Effects of chaotropic and kosmotropic cosolvents on the pressure-induced unfolding and denaturation of proteins: An FT-IR study on staphylococcal nuclease. *Biochemistry* 43, 3336–3345.

(22) Van Eylen, D., Oey, I., Hendrickx, M., and Van Loey, A. (2008) Behavior of mustard seed (*Sinapis alba* L.) myrosinase during temperature/pressure treatments: A case study on enzyme activity and stability. *Eur. Food Res. Technol.* 226, 545–553.

(23) Yamasaki, K., Taniguchi, Y., Takeda, N., Nakano, K., Yamasaki, T., Kanaya, S., and Oobatake, M. (1998) Pressure-denatured state of *Escherichia coli* ribonuclease HI as monitored by Fourier transform infrared and NMR spectroscopy. *Biochemistry* 37, 18001–18009.

(24) Dirix, C., Meersman, F., MacPhee, C. E., Dobson, C. M., and Heremans, K. (2005) High hydrostatic pressure dissociates early aggregates of TTR105-115, but not the mature amyloid fibrils. *J. Mol. Biol.* 347, 903–909.

(25) Taniguchi, Y., Okuno, A., and Kato, M. (2010) Pressure effects on the structure, kinetic, and thermodynamic properties of heat-induced aggregation of protein studied by FT-IR spectroscopy. In *International Conference on High Pressure Science and Technology*, Joint Airtap-22 and Hpcj-50 (Takemura, K., Ed.).

(26) Foguel, B., and Silva, J. L. (2004) New insights into the mechanisms of protein misfolding and aggregation in amyloidogenic diseases derived from pressure studies. *Biochemistry* 43, 11361–11370.

(27) Cordeiro, Y., Kraineva, J., Suarez, M. C., Tempesta, A. G., Kelly, J. W., Silva, J. L., Winter, R., and Foguel, D. (2006) Fourier transform infrared spectroscopy provides a fingerprint for the tetramer and for the aggregates of transthyretin. *Biophys. J.* 91, 957–967.

(28) Meersman, F., Smeller, L., and Heremans, K. (2002) Comparative Fourier transform infrared spectroscopy study of cold-, pressure-, and heat-induced unfolding and aggregation of myoglobin. *Biophys. J.* 82, 2635–2644.

(29) Gross, M., and Jaenicke, R. (1994) Proteins under Pressure: The influence of High Hydrostatic Pressure on Structure, Function and Assembly of Protein Complexes. *Eur. J. Biochem.* 221, 617–630.

(30) Smeller, L. (2002) Pressure-temperature phase diagrams of biomolecules. *Biochim. Biophys. Acta* 1595, 11–29.

(31) Smeller, L., Rubens, P., and Heremans, K. (1999) Pressure effect on the temperature-induced unfolding and tendency to aggregate of myoglobin. *Biochemistry* 38, 3816–3820.

(32) Kitahara, R., Hata, K., Maeno, A., Akasaka, K., Chimenti, M. S., Garcia-Moreno, B., Schroer, M. A., Jeworrek, C., Tolan, M., Winter, R., Roche, J., Roumestand, C., de Guillen, K. M., and Royer, C. A. (2011) Structural plasticity of staphylococcal nuclease probed by perturbation with pressure and pH. *Proteins* 79, 1293–1305.

(33) Taniguchi, Y., Takeda, N., Ado, K., and Maeda, R. (2009) High pressure FT-IR spectroscopic study on the secondary structure changes in insulin amyloid fibril and aggregate. *High Pressure Res.* 29, 676–679.

(34) Meyer-Pittroff, R., Behrendt, H., and Ring, J. (2007) Specific immuno-modulation and therapy by means of high pressure treated allergens. *High Pressure Res.* 27, 63–67.

(35) Houska, M., Heroldova, M., Vavrova, H., Kucera, P., Setinova, I., Havranova, M., Honzova, S., Strohal, J., Kminkova, M., Proskova, A., and Novotna, P. (2009) Is high-pressure treatment able to modify the allergenicity of the main apple juice allergen, Mal d1? *High Pressure Res.* 29, 14–22.

(36) Husband, F. A., Aldick, T., Van der Plancken, I., Grauwet, T., Hendrickx, M., Skypala, I., and Mackie, A. R. (2011) High-pressure treatment reduces the immunoreactivity of the major allergens in apple and celeriac. *Mol. Nutr. Food Res.* 55, 1087–1095.

(37) Fernandez, A., Butz, P., and Tauscher, B. (2009) IgE binding capacity of apple allergens preserved after high pressure treatment. *High Pressure Res.* 29, 705–712.

(38) Somkuti, J., Houska, M., and Smeller, L. (2011) Pressure and temperature stability of the main apple allergen Mal d1. *Eur. Biophys. J.* 40, 143–151.

(39) Barth, A. (2007) Infrared spectroscopy of proteins. *Biochim. Biophys. Acta* 1767, 1073–1101.

(40) Smeller, L., Meersman, F., and Heremans, K. (2006) Refolding studies using pressure: The folding landscape of lysozyme in the pressure-temperature plane. *Biochim. Biophys. Acta* 1764, 497–505.

(41) Smeller, L., Goossens, K., and Heremans, K. (1995) Determination of the secondary structure of proteins at high pressure. *Vib. Spectrosc.* 8, 199–203.

(42) Smeller, L., Meersman, F., Fidy, J., and Heremans, K. (2003) High-pressure FTIR study of the stability of horseradish peroxidase.



Effect of heme substitution, ligand binding,  $\text{Ca}^{2+}$  removal, and reduction of the disulfide bonds. *Biochemistry* 42, 553–561.

(43) Kaposi, A. D., Wright, W. W., Fidy, J., Stavrov, S. S., Vanderkooi, J. M., and Rasnik, I. (2001) Carbonmonoxy horseradish peroxidase as a function of pH and substrate: Influence of local electric fields on the optical and infrared spectra. *Biochemistry* 40, 3483–3491.

(44) Nara, M., and Tanokura, M. (2008) Infrared spectroscopic study of the metal-coordination structures of calcium-binding proteins. *Biochem. Biophys. Res. Commun.* 369, 225–239.

(45) Wong, P. T. T., and Moffat, D. J. (1989) A new internal pressure calibrant for high-pressure infrared spectroscopy of aqueous systems. *Appl. Spectrosc.* 43, 1279–1281.

(46) Smeller, L., Goossens, K., and Heremans, K. (1995) How to minimize certain artifacts in Fourier self-deconvolution. *Appl. Spectrosc.* 49, 1538–1542.

(47) Susi, H., and Byler, D. M. (1986) Resolution-Enhanced Fourier-Transform Infrared-Spectroscopy of Enzymes. *Methods Enzymol.* 130, 290–311.

(48) Arnold, K., Bordoli, L., Kopp, J., and Schwede, T. (2006) The SWISS-MODEL workspace: A web-based environment for protein structure homology modelling. *Bioinformatics* 22, 195–201.

(49) Schwede, T., Kopp, J., Guex, N., and Peitsch, M. C. (2003) SWISS-MODEL: An automated protein homology-modeling server. *Nucleic Acids Res.* 31, 3381–3385.

(50) Guex, N., and Peitsch, M. C. (1997) SWISS-MODEL and the Swiss-PdbViewer: An environment for comparative protein modeling. *Electrophoresis* 18, 2714–2723.

(51) Ismail, A. A., Mantsch, H. H., and Wong, P. T. T. (1992) Aggregation of chymotrypsinogen: Portrait by infrared spectroscopy. *Biochim. Biophys. Acta* 1121, 183–188.

(52) Nara, M., Torii, H., and Tasumi, M. (1996) Correlation between the vibrational frequencies of the carboxylate group and the types of its coordination to a metal ion: An ab initio molecular orbital study. *J. Phys. Chem.* 100, 19812–19817.

(53) Permyakoy, S. E., Bakunts, A. G., Denesyuk, A. I., Knyazeva, E. L., Uversky, V. N., and Permyakov, E. A. (2008) Apo-parvalbumin as an intrinsically disordered protein. *Proteins* 72, 822–836.

(54) Foguel, D., Suarez, M. C., Barbosa, C., Rodrigues, J. J., Sorenson, M. M., Smillie, L. B., and Silva, J. L. (1996) Mimicry of the calcium-induced conformational state of troponin C by low temperature under pressure. *Proc. Natl. Acad. Sci. U.S.A.* 93, 10642–10646.

(55) Rocha, C. B., Suarez, M. C., Yu, A., Ballard, L., Sorenson, M. M., Foguel, D., and Silva, J. L. (2008) Volume and free energy of folding for troponin CC-domain: Linkage to ion binding and N-domain interaction. *Biochemistry* 47, 5047–5058.

(56) Suarez, M. C., Rocha, C. B., Sorenson, M. M., Silva, J. L., and Foguel, D. (2008) Free-Energy Linkage between Folding and Calcium Binding in EF-Hand Proteins. *Biophys. J.* 95, 4820–4828.

(57) Seefeldt, M. B., Rosendahl, M. S., Cleland, J. L., and Hesterberg, L. K. (2009) Application of High Hydrostatic Pressure to Dissociate Aggregates and Refold Proteins. *Curr. Pharm. Biotechnol.* 10, 447–455.

(58) Floriano, W. B., Nascimento, M. A. C., Domont, G. B., and Goddard, W. A. (1998) Effects of pressure on the structure of metmyoglobin: Molecular dynamics predictions for pressure unfolding through a molten globule intermediate. *Protein Sci.* 7, 2301–2313.

(59) Dzwolak, W., Kato, M., Shimizu, A., and Taniguchi, Y. (1999) Fourier-transform infrared spectroscopy study of the pressure-induced changes in the structure of the bovine  $\alpha$ -lactalbumin: The stabilizing role of the calcium ion. *Biochim. Biophys. Acta* 1433, 45–55.

(60) Swoboda, I., Bugajska-Schretter, A., Verdino, P., Keller, W., Sperr, W. R., Valent, P., Valenta, R., and Spitzauer, S. (2002) Recombinant carp parvalbumin, the major cross-reactive fish allergen: A tool for diagnosis and therapy of fish allergy. *J. Immunol.* 168, 4576–4584.